Supplementary Materials for: **Functional Variants in *LRRK2* Confer Pleiotropic Effects on Crohn's Disease and Parkinson's Disease**

Table of Contents

Sample collection

A total of 2,066 individuals with Crohn's disease (CD), and 3,633 unaffected controls were enrolled at 14 centers throughout North America, Europe, and Israel (**Table S3**). All participants were unrelated and self-reported as having Ashkenazi Jewish ancestry and provided written consent for genotyping and analysis, under protocols approved by each site's local institutional review board. IBD patients had diagnoses confirmed at each recruiting site by a health care provider, based on standard criteria including clinical presentation, as well as endoscopic, radiologic and/or pathologic confirmation.

Collection and analysis of exome sequencing data

Exome sequencing and variant calling

Genomic DNA was extracted from whole blood; sheared exomic fragments were captured with the NimbleGen 2.1 M human exome array (Roche/NimbleGen, Madison, WI). We sequenced the captured libraries as paired-end 75-bp reads using Illumina GAII (45 samples, comprising 39 unrelated individuals and 3 sibling pairs) and HiSeq (5 unrelated samples) sequencers, with 8 samples bar-coded per sequencing lane. Sequence reads were mapped to the reference genome (hg18) using the BWA program using default parameters (*59*), and coordinates were translated to the hg19 reference genome using LiftOver in the UCSC Genome Browser with default parameters (*60*). The Genome Analysis Toolkit (GATK) v2 was used to call alleles at variant sites (*61*). Sample-level realignment and multi-sample SNP calling were performed using default parameters and the GATKStandard variant filter. Visual confirmation of insertion-deletion polymorphisms, which have a higher error rate in variant calling, was performed in the Integrative Genomics Viewer (*62*).

Among samples sequenced using GAII sequencers, the average number of reads was 71,876,305, with 42,552,977 (58.8%) of reads on-target (within exomic regions), which yielded an average coverage depth of 91.5X. These individuals each had, on average, 31,493 variants detected with at least one non-reference allele. Samples sequenced by HiSeq had a mean read count of 151,352,500, with 58,934,621 (38.9%) on-target, average coverage depth of 128X, and 44,114 variants detected. The variant sets from both machine types were merged, and no platform stratification was carried forward in the analysis.

Imputation of variants detected by exome sequencing

In order to determine whether the variants identified through our exome sequencing were already tagged in our previous AJ GWAS, we performed imputation and assessed the estimated imputation quality. The GWAS cohort consisted of 907 AJ Crohn's independent disease cases and 1,644 matched controls; individuals with only partial AJ ancestry, which were analyzed in the previous GWAS, were excluded here (*11*). Our exome sequencing samples, which were used in the GWAS analysis, served as a reference panel for imputation on the full case-control cohort, using BEAGLE version 3.3.0 with default parameters (*63*). BEAGLE performs an internal estimation of imputation accuracy (r^2, correlation between imputed and true genotypes). We conducted an additional study of empirical imputation accuracy, stratifying the exome

sequencing markers by minor allele count and BEAGLE estimated accuracy, and then masking 25 randomly selected markers within each group. Pearson correlation between observed and inferred allele dosage was calculated after imputation. We determined that for variants with BEAGLE accuracies above 0.7 and minor allele frequencies over 5%, there was high agreement between the estimated and empirical imputation accuracies. We therefore used MAF $\geq$ 5% and BEAGLE $r^2 \geq 0.7$ as the joint criteria for defining variation already successfully assayed by the GWAS platforms; 8,758 exomic coding variants were defined as well-imputed (**Figure S2**), with all other markers eligible for addition to the HumanExome platform as custom content (**Figure S1**). As a fine-mapping exercise, we performed case-control association analysis among the well-imputed variants and found no evidence for novel CD association signals at a Bonferroni-corrected significance threshold of 10^{-5}.

Custom assay design

HumanExome base content

The Illumina HumanExome beadchip v1.0 contains 230,296 non-synonymous and canonical splice-site markers, located in over 20,000 RefSeq-listed genes that were identified in various large exome-sequencing studies. The largest number of samples was contributed by the NHLBI exome sequencing study (4260), and autoimmune disease samples were represented in the GO type II diabetes (T2D), Hispanic T2D genes, and Pfizer-MGH-Broad T2D study cohorts. The vast majority of samples were of European ancestry, with little Ashkenazi Jewish representation reported. The targeting of predominantly rare coding-region variants unsurprisingly results in a low proportion of genomic variation captured (0.088 of variation with MAF > 1.0% tagged with $r^2 > 0.8$).

Selection of variants as custom content

From the list of candidate non-synonymous variants identified in our exome sequencing, we removed those already included in the HumanExome base content. We then evaluated the markers using the Illumina Assay Design Tool. We eliminated the variants that had a Final Score less than 0.7; this value represents the probability that a probe designed to assay a given variant will be successful. Common background markers tagging previously established IBD loci in an Immunochip-based study were also added to the genotyping platform (*1*). This yielded the final set of variants that was used as custom content on the genotyping platform.

Because the goal of the exome sequencing phase of the study was variant detection, rather than association analysis, the sibling-pair data was not stratified or separated from the unrelated samples. Given the small number of sibling pairs sequenced, we did not perform any linkage-based analysis of these data, nor were we able to assess for specific variants that were differentially carried by familial and sporadic CD cases.

Selection of variants and samples for analysis

Genotype and sample quality filtering

Genotyping data were collected at three genotyping centers (Philadelphia, PA, Manhasset, NY, and Los Angeles, CA) using the same custom genotyping array. The data were combined and preliminary genotypes were called jointly using input from all three centers in GenomeStudio. Following guidelines produced by the Cohorts for Heart and Aging Research in Genome Epidemiology (CHARGE) consortium, we enforced quality control using SNP metrics based on fluorescent probe intensities and genotype frequencies, as well as visual inspection of markers with uncertain genotyping quality (*48*). First, samples with low quality metrics (genotype call rate < 0.96 and/or $p10_{GC} < 0.4125$) were removed, and the markers re-clustered in GenomeStudio. Markers with overall low probe intensity were removed. A subset of SNPs was excluded based on meeting any of these genotype clustering criteria:

- Θ_{AA} mean ≥ 0.25
- Θ_{BB} mean < 0.8
- Θ_{AB} mean < 0.19 and ≥ 0.83
- Θ_{AA} deviation > 0.0355
- Θ_{BB} deviation > 0.0355
- Θ_{AB} deviation < 0.0107 and ≥ 0.08
- Cluster separation < 0.35
- Heterozygote excess < -0.2 and > 0.03
- For chromosome X only: Heterozygote excess < -0.6
- $R_{mean}(AA)$, $R_{mean}(AB)$, or $R_{mean}(BB) < 0.2$
- Call rate < 0.99

Another set of SNPs was flagged for manual review by the following criteria. During manual review, genotype cluster boundaries were adjusted to optimize cluster separation and genotype call rate.

- Θ_{AA} mean 0.15 to 0.25
- Θ_{BB} mean 0.8 to 0.9
- Θ_{AB} mean 0.19 to 0.28 and 0.78 to 0.83
- Θ_{AA} deviation 0.027 to 0.0355
- Θ_{BB} deviation 0.027 to 0.0355
- Θ_{AB} deviation 0.046 to 0.08
- Cluster separation 0.35 to 0.45
- Heterozygote excess -0.055 to -0.2 and 0.017 to 0.03
- For chromosome X only: Heterozygote excess > 0
- $Frequency_{AB} \geq 0.508$
- $R_{mean}(AA)$, $R_{mean}(AB)$, or $R_{mean}(BB)$ 0.2 to 0.25
- Call frequency 0.99 to 0.999

- All chromosome Y
- All chromosome MT
- Rep errors > 0

An additional set of variants were flagged as potentially having a mis-called heterozygote cluster. These markers, defined by the criteria below, were also manually reviewed.

- $Frequency_{AB} = 0$ and $frequency_{AA} > 0$ and $frequency_{BB} > 0$
- $Frequency_{AA} = 1$ and call frequency < 1
- $Frequency_{BB} = 1$ and call frequency < 1
- $Frequency_{AB} = 0$ and MAF > 0

After all manual review was completed, additional quality thresholds for sample exclusion (genotype call rate < 0.968, $p50_{GC} < 0.758$, or average heterozygosity > 0.31) were applied. We observed no differences between genotyping centers in the quality statistics. Related samples were identified using pairwise identity-by-descent detection in PLINK (*64*) and removed. Samples with discrepancy between self-reported gender and genotypic gender were excluded. Following association analysis, cluster plots of the 198 significant coding markers were re-examined to ensure high-quality genotype calling.

Among all genotyped non-synonymous markers, 19,361 markers were removed by genotype quality filtering, and 153,978 were monomorphic in the AJ cohort, which yielded the final set of 61,234 markers for analysis (**Figure S1**).

Principal components analysis

We created a set of 10,312 null independent autosomal polymorphisms by removing markers with pairwise linkage disequilibrium (LD) of $r^2 > 0.05$, those with minor allele frequency (MAF) below 0.05, custom content, and variants within established IBD loci. Principal components analysis (PCA) was performed using the princomp() function in R version 2.15.1 (**Figure S3**). The PCA was conducted on our dataset in conjunction with a reference cohort comprising currently unpublished, non-Jewish European-ancestry samples on which exome chip data was available. Boundaries defined along the top three principal components were used to define outlier samples for removal from the AJ cohort. We determined that many of the excluded samples had self-reported less than 100% AJ ancestry. No significant correlations between the top principal components and case-control status, geographic location, or genotyping center were observed. Using membership in the PCA cluster as genetic validation of AJ ancestry, we conducted all further analyses using only samples with 100% AJ ancestry: 1,477 CD cases, and 2,614 independent healthy controls (**Table S3**). Because we excluded recent ancestry-admixed subjects and the AJ population is a homogenous isolate, we did not include population substructure as an additional covariate in downstream analyses, in order to maximize our power to detect rare-variant association signals.

Association testing

Power calculations

For the exome sequencing phase of our study, we performed power calculations using binomial distribution probability estimates (**Table S1**). Because the cohort consisted of 44 independent CD cases and 3 pairs of siblings, the calculation was performed assuming 97 independent chromosomes. For the association testing power estimates, we used cumulative probability densities under a normal distribution.

Quantile-quantile (Q-Q) plots

We created a Q-Q plot of chi-square association statistics (**Figure S4**) using a reduced set of non-synonymous variants in order to assess the validity of the null distribution assumption throughout our exomic dataset. We removed markers with high pairwise linkage disequilibrium ($r^2 \geq 0.5$) or with a minor allele count of 1, since, given our study's sample size, such low-frequency variants could not achieve significance ($P < 0.05$) even without any correction for multiple testing. Genomic inflation was calculated using this dataset and found to be within the standard range of previous GWA studies ($\lambda = 1.095$).

Evaluation of conditional independence

Logistic regression, in which coding variants and background associated markers served as covariates, was used to define independent association signals. Conditionally dependent pairs of variants were defined as those whose conditioned P-values were at least an order of magnitude less significant than the individual single-point P-values (in logistic regression with no covariates).

Non-additive association and epistasis

In single-point analysis, none of the associated markers showed deviation from standard allelic (additive) association (**Table S4**, "Alternate models" tab), and there was no evidence of interaction effects between any of the nominally significant variants.

Association with age of onset and Crohn's disease location

Crohn's disease age of diagnosis was available for 6,095 CD cases, and disease location was available for 5,775 CD cases, using data from both AJ and NJ individuals in the NIDDK IBDGC repository database. Association testing for these two phenotypes was performed using linear regression and chi-square testing, respectively.

Selection of markers for trends among independent highly associated markers

To evaluate for significant patterns among the markers highly associated with CD, we performed LD pruning (pairwise $r^2 < 0.5$) to create a set of independent polymorphisms. From these, we used the set of 100 most associated markers ($P < 1.3 \times 10^{-3}$) to perform several analyses described in the following three sections.

Imputation of *LRRK2* locus variants in CD and PD cohorts

Sample selection

We expanded our analysis to evaluate all polymorphisms, including noncoding variation, throughout the 5 Mb-region on chromosome 12 symmetrically flanking *LRRK2*, in analysis of individuals with CD or PD, as well as in comparable non-Jewish European ancestry samples whose ancestry was validated using principal component analysis as previously described (*65*). Additional healthy control genotypes from the 1,000 Genomes Project representing independent individuals from the CEU and TSI populations were extracted from the Phase 1 data release (11/23/2010) and included single-nucleotide polymorphisms (SNPs) and short indels (*66*). Genotypes from the Ashkenazi Genome Consortium (TAGC) representing healthy controls of AJ ancestry were extracted from the public Phase 1 release (9/9/2014, http://browser.1000genomes.org) and also included both SNPs and short indels (*67*).

Imputation of genotypes

In the process of combining data from the various sources described above, we ensured that the datasets had consistent strand alignment and variant positions. Markers that were exclusive to the whole-genome sequencing datasets (TAGC and 1,000 Genomes for the AJ and NJ analyses, respectively) were omitted to increase overall imputation accuracy, as we did not treat these as reference datasets for imputation, given their relatively small number of individuals included. A total of 4,124 variants were used as imputation input in the AJ data, compared to 2,256 markers used for imputation in NJs; this discrepancy was due to a greater variety of genotyping platforms (and therefore a larger set of genotyped markers) used in the AJ datasets (**Table S2**). Reference-free imputation was performed using MACH, with 300 haplotype states and 50 Markov chain rounds (*50*). Integrated imputation of CD, PD, and control samples was performed in a single process, with no phenotype data used as input for the algorithm. The AJ and NJ datasets were imputed separately to reduce runtime, and only variants with high imputation quality ($R^2 > 0.7$) were retained, which yielded 1,436 Ashkenazi and 643 non-Jewish polymorphisms, including 486 overlapping variants present in both populations' datasets (**Figure S1**). We noted that imputation quality was generally better in the Jewish data than in NJ, indicating a greater extent of haplotype sharing in the AJ population, which is consistent with previous population genetic studies (*67*).

Association analysis

Within each population, we conducted separate association analyses for CD and PD. P-values were calculated using logistic regression in order to facilitate direct comparison between unconditioned analysis and those which included certain markers as covariates. As in the first stage analysis focused on novel non-synonymous variation, we again did not use population stratification as a covariate in AJ analyses, noting that previous work has shown that there exists little intra-Ashkenazi population structure using PCA. This prior study demonstrated that the first PC in AJs is already a local signal (human leukocyte antigen, or HLA), not a genome-wide one, implying that there is no room for stratification correction with PCs (*68*). As genome- or exome-wide data were not obtained on many NJ samples, PCA was unable to be performed for that analysis.

Healthy controls were randomly assigned to either CD or PD analysis, to ensure independence of the analyses; using only a subset of controls to estimate each set of association statistics accounted for minor discrepancies in the ORs and P-values for the *LRRK2* variants reported in **Tables 1 and 2**.

Comparisons of overall genetic architecture between CD and PD (as in **Figure 3**) were made using an LD-pruned set of markers (26 markers in the AJ data; 29 in NJ), in which variant pairs with high LD ($r^2 > 0.8$) had been eliminated.

Experimental Studies

Autophagy experiments in human macrophages

Peripheral Blood Mononuclear Cells (PBMC) were isolated from approximately 50mL of forearm vein blood using Cell Preparation Tube (BD Vacutainer® CPT™) with Sodium Heparin (362753) per manufacturer's protocol. PBMCs were incubated in a nunclon delta 6-well plate for 90 minutes in Monocyte Attachment Medium (MAM) (C-28051, promocell, Heidelberg, Germany) at 37 degrees Celsius and 5% of CO2. Then cells were washed twice using MAM and monocytes remained attached. Two milliliters of complete M1 macrophage generation medium purchased from Promocell were added per well. Complete M1 medium included the basal M1 medium (C-28055, Promocell, Heidelberg, Germany) plus supplement mix M1-macrophage generation medium DXF (c-39855, promocell, Heidelberg, Germany) plus M1 cytokine mix (c-39894, Promocell, Heidelberg, Germany). At day 6, one milliliter of complete M1 macrophage medium was added to each well. At day 10, the medium was changed and replaced with fresh complete M1 macrophage medium. At day 12, matured M1-macrophages were incubated in PBS and in complete M1 macrophage medium for 45 minutes. M1-macrophages from these patients were derived from whole peripheral blood monocytes according to the manufacturer's instructions (Promocell, Heidelberg, Germany). Monocytes were polarized to mature M1-macrophages in the DXF M1-macrophage generation medium (M1-medium, resting condition, Promocell) for 12 days and then incubated in PBS and M1 medium for 45 minutes. Cells were then lysed in RIPA buffer (PI89900, Thermo Scientific, Waltham, MA USA) with Halt Protease and Phosphatase Inhibitor Cocktail (PI78440, Thermo Scientific, Waltham, MA USA). Ten micrograms of total protein were loaded onto 4-12% Bis-Tris Plus precast SDS-polyacrylamide

gels, transferred onto a PVDF membrane and probed with primary rabbit anti-LRRK2 antibody (ab133474, abcam), mouse anti-acetylated alpha-tubulin (T7451, Sigma-Aldrich, St. Louis, MO), rabbit anti-alpha tubulin (ab4074, abcam), mouse anti-SQSTM1 (sc-28359, Santa Cruz Biotechnology), and rabbit anti-LC3B (NB100-2220, Novus Biologicals). The corresponding HRP-conjugated secondary antibody was applied for detection. Total alpha-tubulin was used as a loading control for normalization and protein densitometry was performed using ImageJ software. LRRK2 degradation was assessed as the ratio of degraded LRRK2 to total LRRK2 (full length + degraded) protein. Alpha-tubulin acetylation was assessed as the ratio of acetylated to total alpha-tubulin.

Supplementary figures

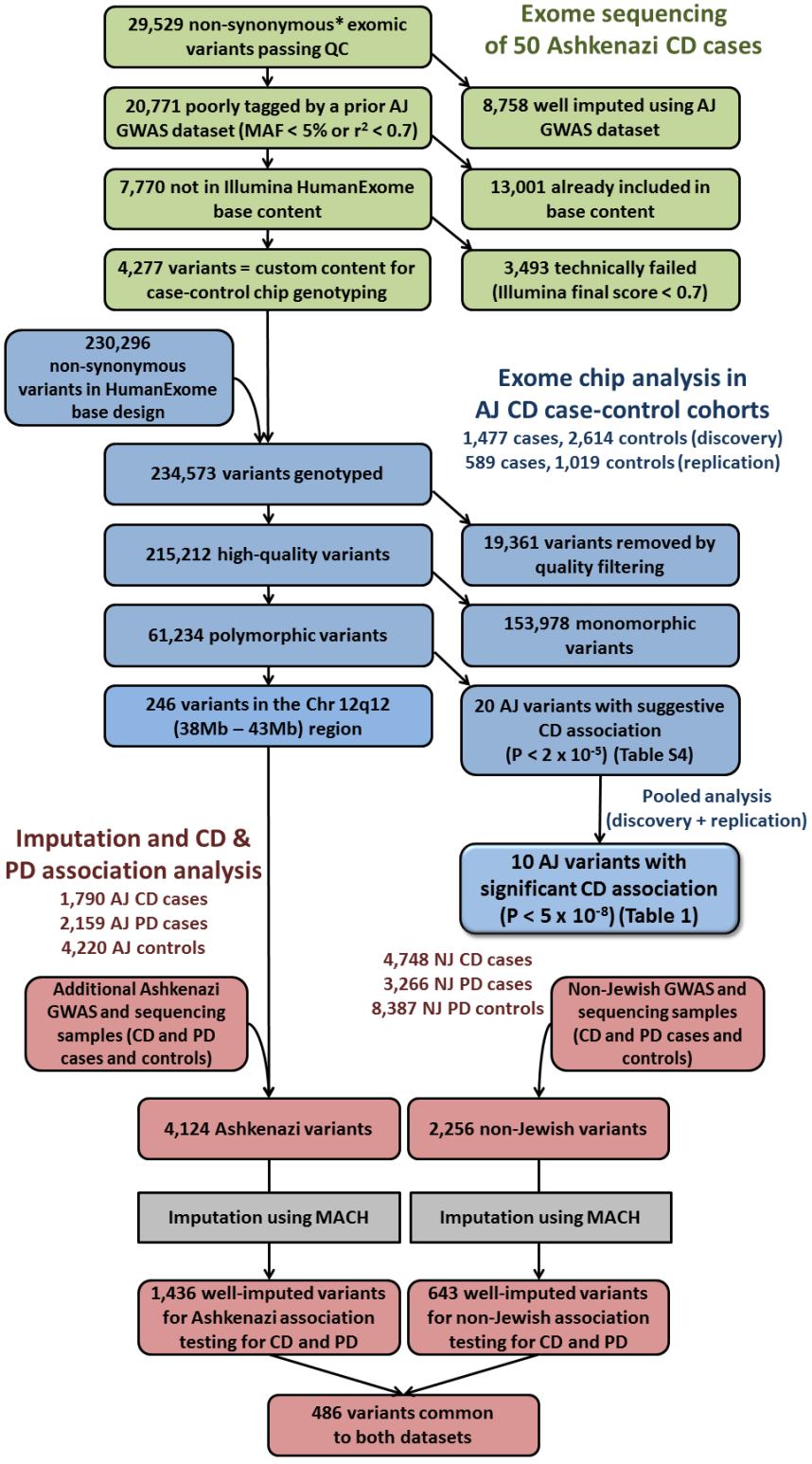

Figure S1: Schematic workflow of genetic analysis, by analytic stages

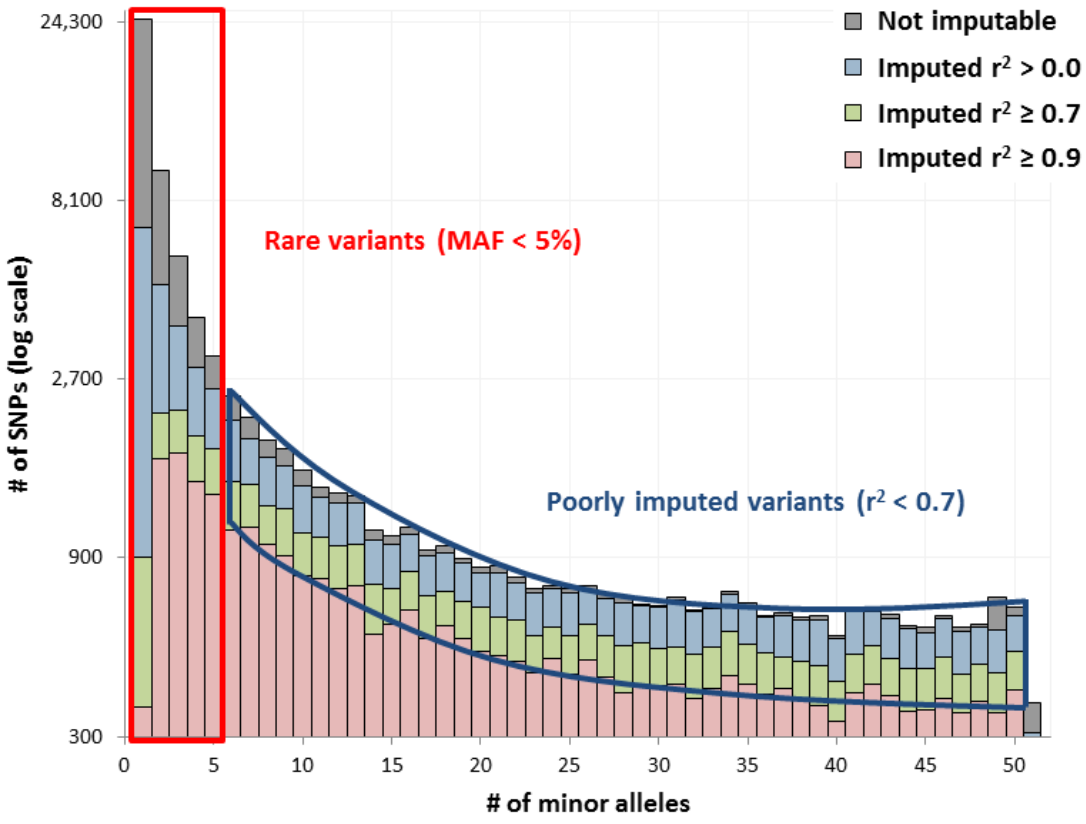

Figure S2: Variants identified through exome sequencing, by MAF and imputation quality.

Colored boxes represent two classes of candidate variants considered for direct genotyping in a case-control cohort: rare variants (red), and common variants with low imputation quality (blue).

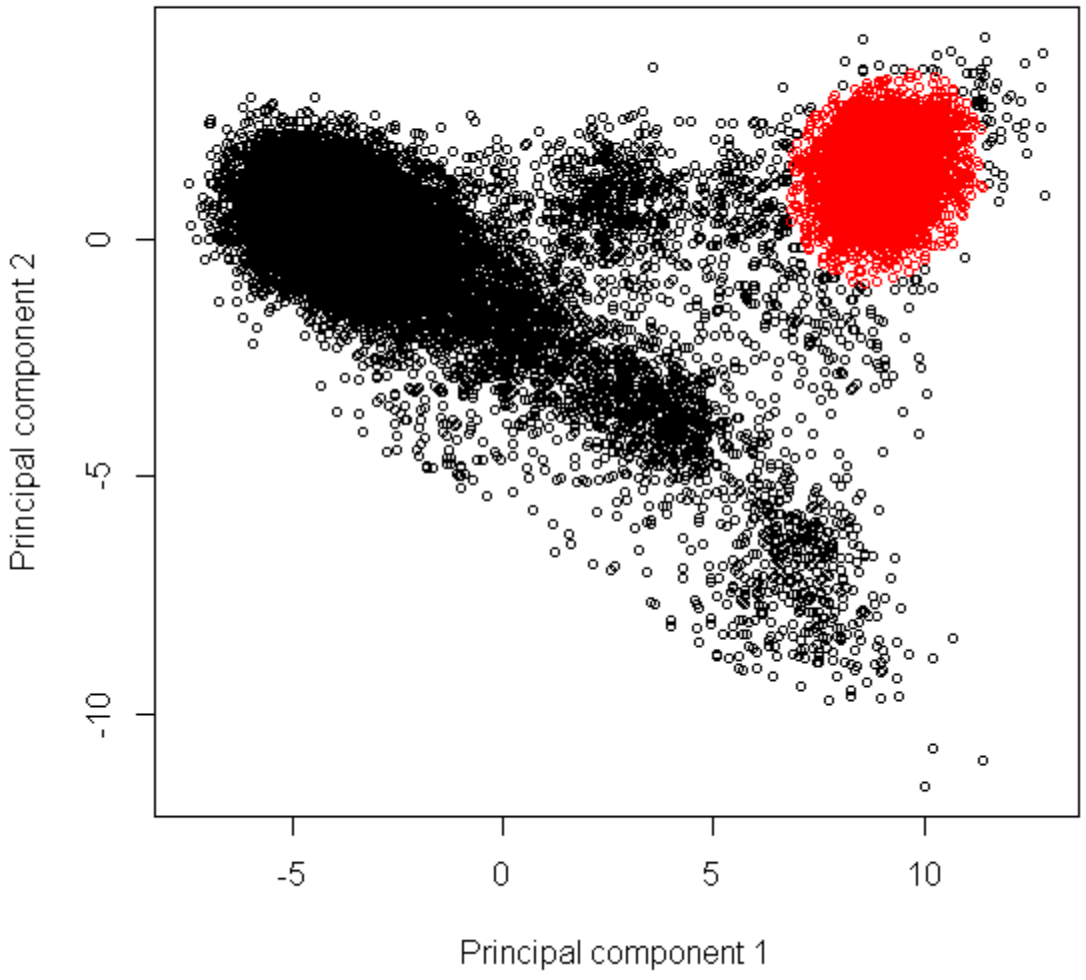

Figure S3: Principal components analysis

Samples defined as having full AJ ancestry are denoted in red.

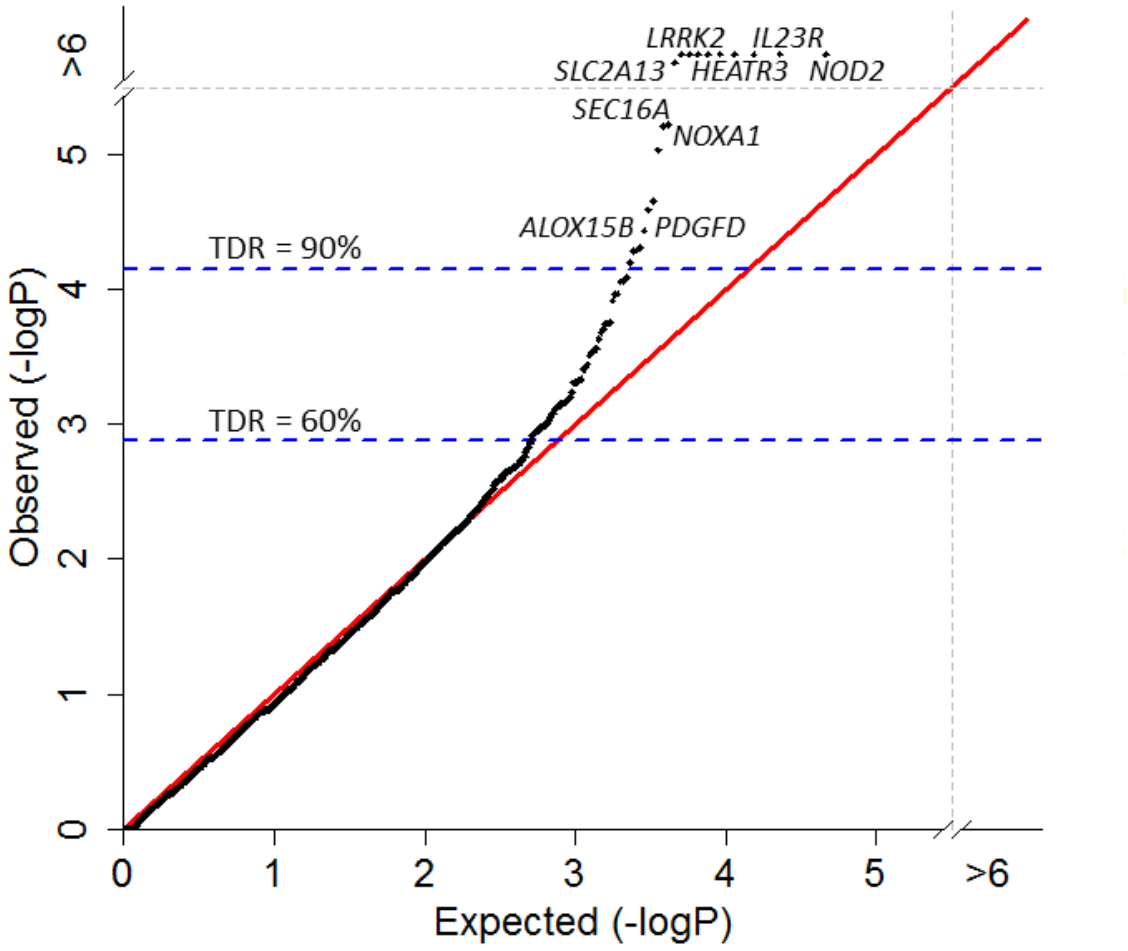

Figure S4: Q-Q plot of CD association results show enrichment of true positive signals below 10^{-3}.

True discovery rate as a function of P-value threshold; the expected numbers of significant markers under the null distribution were calculated through permutation. Blue dotted lines in panels A and B indicate P-value cutoffs corresponding to true discovery rates of 60% and 90%.

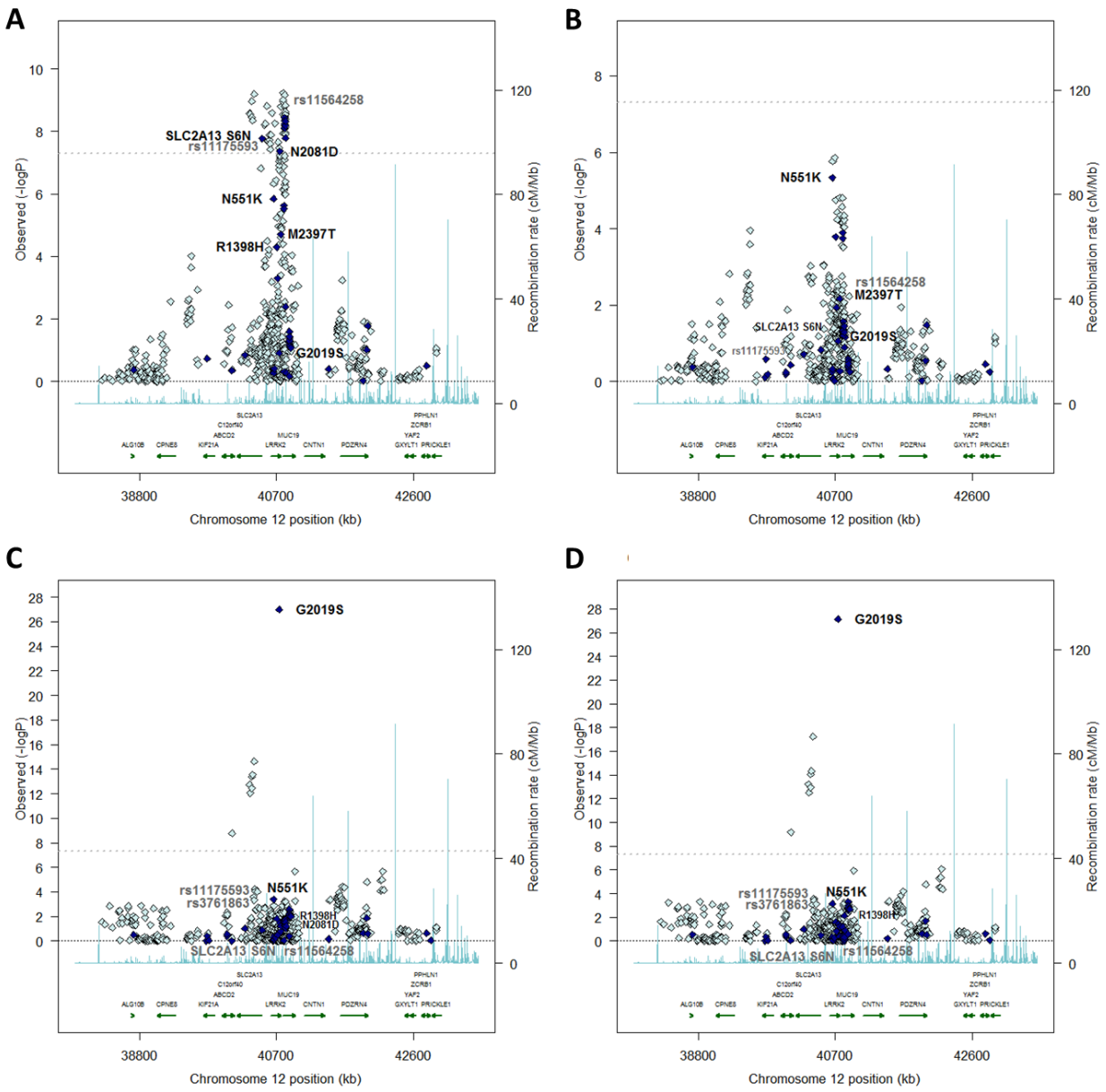

Figure S5: Single-point association with CD and PD in the AJ cohort using imputed genotypes within the *LRRK2* locus, conditioned and unconditioned on the CD-associated coding variant N2081D.

A. Unconditioned analysis of AJ CD. **B.** AJ CD analysis conditioned on N2081D genotypes. **C.** Unconditioned analysis of AJ PD. **D.** AJ PD analysis conditioned on N2081D genotypes. Dark points indicate non-synonymous variants.

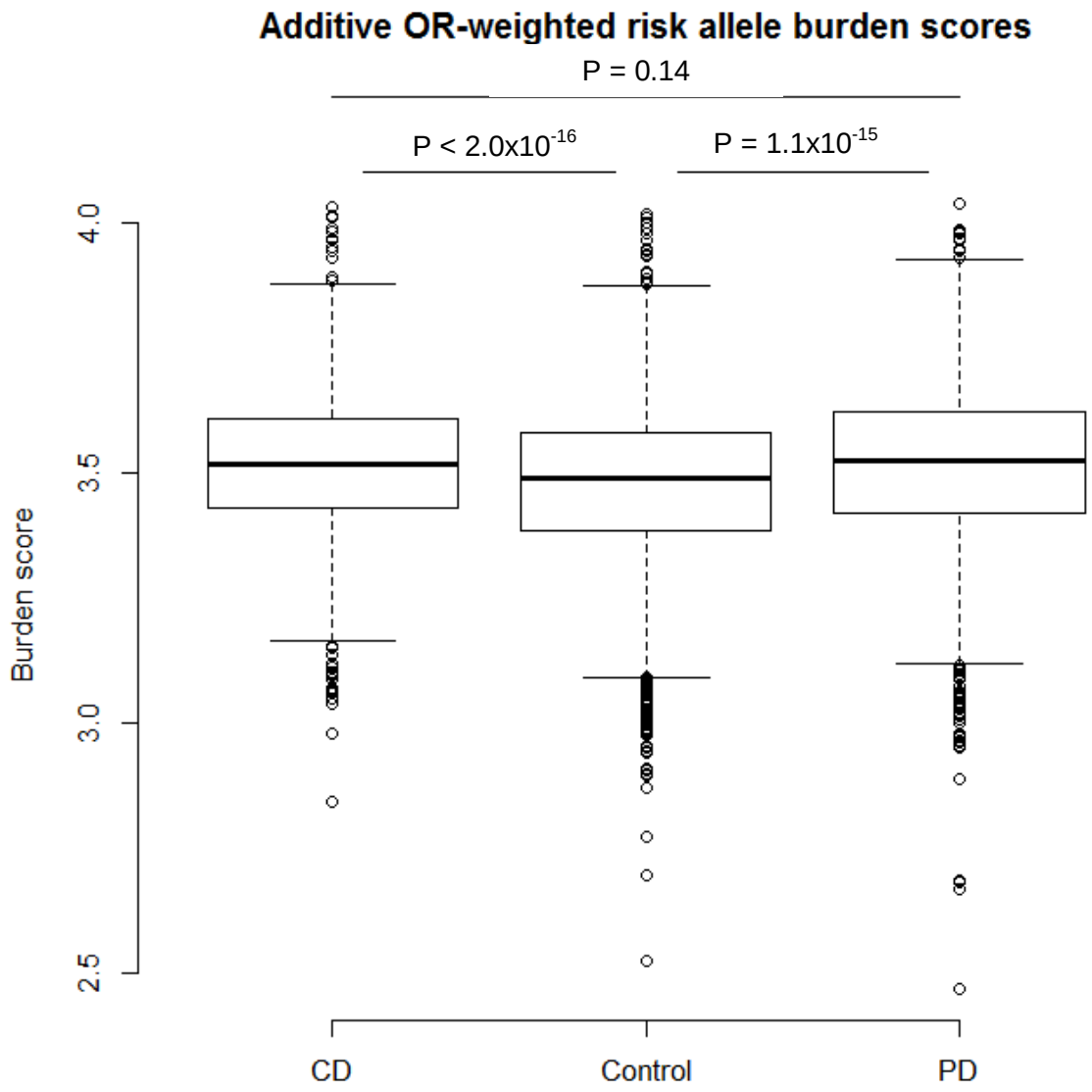

Figure S6: Log odds ratio-weighted additive risk allele burden scores.

The burden scores across the *LRRK2* risk alleles are significantly higher both CD and PD individuals compared to controls, indicating an overall similar genetic architecture throughout the *LRRK2* locus underlying both diseases. Pairwise two-sided *t*-test P-values are shown above the boxplots.

Supplementary tables

	Minor allele frequency (MAF) in case samples										
	0.0001	**0.001**	**0.005**	**0.01**	**0.015**	**0.02**	**0.025**	**0.03**	**0.04**	**0.05**	**0.1**
	Estimated power to detect a variant in sequencing of 97 independent chromosomes, by MAF										
	0.01	0.09	0.39	0.62	0.77	0.86	0.91	0.95	0.98	0.99	1.00

Odds ratio	Estimated Power to Detect Significance (α=0.001) of Single Markers in 1477 Cases and 2614 Controls, by MAF										
0.33	0.00	0.12	0.92	1.00	1.00	1.00	1.00	1.00	1.00	1.00	1.00
0.4	0.00	0.05	0.66	0.97	1.00	1.00	1.00	1.00	1.00	1.00	1.00
0.5	0.00	0.02	0.25	0.65	0.89	0.97	0.99	1.00	1.00	1.00	1.00
0.66	0.00	0.00	0.03	0.11	0.21	0.33	0.46	0.57	0.76	0.87	1.00
0.9	0.00	0.00	0.00	0.00	0.00	0.00	0.01	0.01	0.01	0.01	0.03
1.1	0.00	0.00	0.00	0.00	0.00	0.00	0.00	0.00	0.01	0.01	0.02
1.5	0.00	0.00	0.01	0.04	0.08	0.13	0.19	0.26	0.41	0.55	0.93
2	0.00	0.01	0.06	0.19	0.36	0.54	0.69	0.80	0.93	0.98	1.00
2.5	0.00	0.01	0.11	0.36	0.62	0.81	0.91	0.96	1.00	1.00	1.00
3	0.00	0.01	0.17	0.51	0.78	0.92	0.98	0.99	1.00	1.00	1.00

0% power to observe variant	100% power to observe variant
0% power to detect significant association	100% power to detect significant association

Table S1: Power Calculations

4,277	**Total exomic coding variants**
3,702	Missense substitutions
84	Nonsense substitutions
63	Splice variants
3,849	**Total single-nucleotide polymorphisms (SNPs)**
224	Frameshift mutations
204	In-frame indels
428	**Total indels**

Table S2: Ashkenazi Jewish-enriched exomic variants genotyped as custom content

AJ CD exome chip cohorts

Discovery

Cohort	CD	Control	Genotyping/sequencing platform
NIDDK IBDGC	323	89	Illumina HumanExome
ISSMS	352	51	
Yale University	268	-	
Cedars Sinai Medical Center	384	407	
Hebrew University of Jerusalem	-	1579	
Other	150	488	
Total	1477	2614	

Replication

Cohort	CD	Control	Genotyping/sequencing platform
NIDDK IBD GC	74	187	Illumina HiSeq
ISSMS	272	704	Illumina HiSeq
University College London	243	-	Illumina HiSeq
The Ashkenazi Genomic Consortium	-	128	Complete Genomics
Total	589	1019	

Imputation cohorts

Ashkenazi Jewish

Cohort	CD	PD	Control	Genotyping/sequencing platform
NIDDK IBDGC, ISSMS, CSMC, et al.	1477	-	2614	Illumina HumanExome
	313	-	206	Illumina HiSeq
Ashkenazi Jewish PD GWAS	-	1012	669	Affymetrix 550K, Affymetrix 6.0
	-	1095	805	Illumina 660k, Illumina Omni 1M
Hussman Institute of Human Genomics	-	22	15	Illumina Human610
NeuroGenetics Research Consortium	-	88	41	Illumina Omni1 Quad
PROGENI/GenePD	-	87	30	Illumina HumanCNV370
The Ashkenazi Genome Consortium	-	-	128	Complete Genomics
Total	1790	2304	4220[a]	

Non-Jewish European Ancestry

Cohort	CD	PD	Control	Genotyping/sequencing platform
NIDDK IBDGC	4748	-	4829	Illumina HumanExome
Hussman Institute of Human Genomics	-	563	603	Illumina Human610
NeuroGenetics Research Consortium	-	1893	1943	Illumina Omni1 Quad
PROGENI/GenePD	-	810	832	Illumina HumanCNV370
1000 Genomes CEU+TSI	-	-	180	Illumina GAII, Illumina HiSeq
Total	4748	3266	8387	

[a] Total is less than the sum of component study sample numbers due to sample overlap between studies

NIDDK IBDGC = National Institute of Diabetes and Digestive and Kidney Diseases Inflammatory Bowel Disease Genetics Consortium;

ISMMS = Icahn School of Medicine at Mount Sinai; CSMC = Cedars-Sinai Medical Center

CD, Crohn's disease; PD, Parkinson's disease, Control, unaffected individuals.

Table S3: Sample cohorts description

Table S4: All variants with AJ CD discovery P-values < 2 x 10^{-5}

Provided as a supplementary Excel file. The "Alternate models" tab shows results for χ^2-based models of association (Cochran-Armitage trend test, dominant allele, recessive allele, genotypic effect).

Haplotype	$Freq_{CD}$ (%)	$Freq_{control}$ (%)	P-value
N551/**2081D**/**M2397**	8.20	4.87	1.72×10^{-9}
N551/N2081/**M2397**	37.0	34.6	3.17×10^{-2}
551K/N2081/2397T	6.31	9.70	1.64×10^{-7}
N551/N2081/2397T	48.5	50.9	4.46×10^{-2}

Discovery cohort only; bold indicates minor alleles

Table S5: *LRRK2* phased haplotype association

Table S6: All imputed variants with nominal CD or PD association (P < 0.05) within the *LRRK2* region.

Provided as a supplementary Excel file.